



OPEN

## Leveraging the multi-trait donor *Pusa Srijan* for biofortification and yield improvement in bread wheat

Naresh Kumar Bainsla<sup>1</sup>  , Indu Chopra<sup>2</sup> , Vijay Pooniya<sup>3</sup>, Kamal Batra<sup>4</sup> , Prashanth Babu<sup>1</sup>, Sanjay Kumar Singh<sup>1</sup>, Neethu Mohan<sup>1</sup>, Bhavya Beera<sup>1</sup>, Shreetu Singh<sup>1</sup>, Anju Mahendru Singh<sup>1,5</sup> & Rajbir Yadav<sup>1</sup>

Improving grain nutrition without reducing yield remains a key challenge in wheat breeding. *Pusa Srijan* (PS), a tall lodging-tolerant genotype rich in iron (Fe) and zinc (Zn), was evaluated for its potential as a donor to combine nutritional quality with agronomic performance. Families developed from PS were examined across two generations to track genetic progress for yield, grain size, and protein and micronutrient traits. Clear genetic gains were achieved, with grain yield increasing by approximately  $0.8 \text{ t ha}^{-1}$  and thousand-grain weight by 3–4 g from  $F_5$  to  $F_7$ , while Fe and Zn concentrations were maintained at high levels. Variation among families was significant for all traits, and the heritability of Fe and Zn was high, indicating a strong potential for further selection. The relationships among traits showed that Fe contributed positively to yield, allowing micronutrient improvement without compromising productivity. Several PS-derived families combined yielded above  $7 \text{ t ha}^{-1}$  with Fe > 45 ppm and Zn > 40 ppm, demonstrating simultaneous enhancement of yield and grain nutrition. These findings establish *Pusa Srijan* as a valuable donor for breeding high-yielding and nutritionally enriched wheat varieties, contributing to the long-term goal of improving food and nutritional security.

**Keywords** Biofortification, Bread wheat, Iron, Grain quality, Selection index, Zinc

Wheat (*Triticum aestivum* L.) is a cornerstone of global food and nutrition security, supplying a large proportion of daily calories and proteins. Even modest nutritional gains in wheat can have a meaningful impact on public health<sup>1–3</sup>. Malnutrition due to lower micronutrient levels, particularly iron (Fe) and zinc (Zn) deficiencies, is widespread across agro-ecological regions, motivating biofortification as a cost-effective, population-level intervention. Over the past decade, coordinated breeding efforts have streamlined Fe and Zn enrichment in wheat while preserving its agronomic performance<sup>4–8</sup>. Simultaneously improving grain yield with protein and mineral density remains a formidable challenge because of the well-documented trade-offs among these traits. Yield is often negatively correlated with grain protein, whereas its relationship with Fe and Zn varies from neutral to antagonistic, depending on the sink–source balance, environment, and management practices<sup>9–14</sup>. These complexities highlight the need for multivariate breeding strategies that account for trait covariances, rather than targeting single traits independently. Selection indices and discriminant approaches offer a quantitative framework for weighting correlated traits and integrating them into a single composite criterion that ensures a predictable response to selection, particularly when supported by robust inferences on direct and indirect effects. Such analytical tools provide a practical foundation for optimizing multi-trait improvements in biofortification-oriented wheat breeding<sup>15–17</sup>. Genetic mapping and diversity studies have shown sufficient diversity and genetic variation in Fe, Zn, and protein to support the selection and transfer of these traits in adapted backgrounds<sup>3,5</sup>.

Standability is the second but equally practical constraint in wheat. Lodging reduces light interception and harvestable yield and complicates the mechanized operations. Ideotypes for lodging tolerance emphasize culm wall thickness and diameter, basal internode strength, peduncle robustness, root anchorage, and an appropriate height that sustains biomass without excessive leverage<sup>18–23</sup>. Root architectural traits also contribute to stability

<sup>1</sup>Division of Genetics, ICAR- Indian Agricultural Research Institute, New Delhi 110012, India. <sup>2</sup>Division of Soil Science and Agricultural Chemistry, Indian Agricultural Research Institute, New Delhi 110012, India. <sup>3</sup>Division of Agronomy, Indian Agricultural Research Institute, New Delhi 110012, India. <sup>4</sup>Division of Computer Applications, Indian Agricultural Statistics Research Institute, New Delhi 110012, India. <sup>5</sup>ICAR-National Bureau of Plant Genetic Resources, New Delhi 110012, India.  email: bainsla.breeder.icar@gmail.com; tinaindu@gmail.com; bat.kam@gmail.com

and resource capture in diverse soils<sup>24–26</sup>. Among the donor sources available in Indian wheat, *Pusa Srijan* (PS) represents a unique genotype that combines nutritional enrichment with structural resilience. Developed through the intermating of transgressive segregants from NW6049/HD3059 and NW6049/HD2329, followed by pedigree selection to F<sub>8</sub>, PS integrates high grain protein, Fe, and Zn with a tall, robust architecture (~ 140 cm). The genotype exhibits stout basal internodes, a strong peduncle, and thick culm walls, which confer lodging tolerance and support higher biomass. Its straw possesses smooth internodes and high tensile strength, rendering it suitable for biodegradable straw fabrication and other value-added applications<sup>27,28</sup>. These combined features position PS as an important pre-breeding resource that aligns with modern ideotypes emphasizing dual-purpose value—high-yield, nutrient-rich, and environmentally sustainable wheat. Despite its favorable combination of nutritional and structural traits, the contribution of *Pusa Srijan* as a donor for the concurrent enhancement of Fe, Zn, and yield components has not been systematically quantified. Earlier studies have primarily characterized PS at the phenotypic level, with limited evaluation of its genetic behavior across different selection cycles and environments. Understanding the extent to which PS-derived families maintain or improve target traits through successive generations is crucial for effectively integrating them into mainstream breeding programs.

Accordingly, the present study aimed to (i) quantify the distributional shifts in yield, grain quality, and micronutrient traits across the F<sub>5</sub>–F<sub>7</sub> generations; (ii) estimate realized genetic response and stability of key traits; (iii) elucidate inter-trait relationships through correlation, regression, and path analyses; and (iv) assess multivariate structuring of PS-derived families to identify superior genotypes combining biofortification and agronomic performance.

## Materials and methods

### Plant materials and pedigree

Breeding populations were developed using *Pusa Srijan* (PS) as the donor. PS originated from inter-mating transgressive segregants of NW6049/HD3059 and NW6049/HD2329, followed by pedigree selection to F<sub>8</sub> generation. This line combines high grain protein, Fe, and Zn concentrations with tall stature, strong basal internodes, and lodging tolerance<sup>23,28</sup>.

PS was crossed with high-yielding genotypes from station trials, national nurseries, and released varieties to generate experimental families. Both simple and complex crosses were used to integrate the yield potential with nutritional. The pedigree information is given in (Supplementary Table 1). Selection for disease resistance was conducted in F<sub>2</sub>, and the selected plants were bulked to advance F<sub>3</sub>–F<sub>4</sub>. Morphologically superior and resistant plants in F<sub>4</sub> were grown as individual plant families in F<sub>5</sub>. A multi-trait selection index (grain yield, grain weight, Fe, Zn, and protein) guided advancement through ear-to-row F<sub>6</sub> and row-to-plot F<sub>7</sub> testing. HD3385 and *Pusa Srijan* served as Commercial and Parental checks, respectively.

The seeds and plant materials used in the present study were developed and maintained at the Division of Genetics, ICAR-Indian Agricultural Research Institute (IARI), New Delhi, India.

### Experimental sites and seasons

Field experiments were conducted at the Indian Agricultural Research Institute (IARI), New Delhi (28°38' N, 77°09' E; 228 m a.s.l.), during the 2023–24 (F<sub>5</sub>) and 2024–25 (F<sub>7</sub>) rabi seasons under irrigated conditions. The F<sub>6</sub> generation was advanced off-season (June–September 2024) at the ICAR-IIWBR Regional Station, Lahaul & Spiti, Himachal Pradesh (≈ 32°30' N, 76°59' E 3045 m a.s.l.), which serves as a natural hotspot for yellow rust and facilitates rapid generation advancement.

### Experimental design and layout

The F<sub>5</sub> families were evaluated using an augmented design with repeated checks. Each plot measured 4 m × 1.2 m (six rows with 20 cm spacing) and was sown at a seeding rate of 100 kg ha<sup>-1</sup>.

**Ear-to-row advancement** Selected single plants from superior F<sub>5</sub> plots were harvested as individual ears and grown as *ear-to-row* progenies in F<sub>6</sub> at the Lahaul & Spiti site. Rows showing rust infection or poor uniformity were removed.

**Row-to-plot evaluation** Uniform and rust-free F<sub>6</sub> rows were bulked within families and evaluated as *row-to-plot* progenies in F<sub>7</sub> at IARI, New Delhi, using the same augmented design as described above.

This design ensured continuity of selection pressure across generations and enabled the assessment of realized genetic gain and family stability.

### Soil characteristics and crop management

At IARI, the soil is a moderately alkaline sandy loam with pH 7.5–8.5 and EC 0.4–0.6 dS m<sup>-1</sup>, low organic C (0.41%), and available nutrients at 0–15 cm of N < 280 kg ha<sup>-1</sup>, P 25–30 kg ha<sup>-1</sup>, and K 120–280 kg ha<sup>-1</sup>. A recommended N: P:K dose of 150:60:40 kg ha<sup>-1</sup> and zinc fertilizer as ZnSO<sub>4</sub> 5.25 kg ha<sup>-1</sup> were applied uniformly. Trials followed standard crop management practices of irrigated management (three assured irrigations complemented by natural rainfall events during the growth periods) and plant protection practices.

### Phenotyping and laboratory assays

The measured traits included grain yield (t ha<sup>-1</sup>), thousand-grain weight (TGW; g), grain protein (%), iron (Fe; ppm), and zinc (Zn; ppm). Trait evaluation followed standardized protocols adapted from the ICAR-IARI and CIMMYT biofortification laboratories to ensure reproducibility and comparability across the years.

### Grain yield and yield components

Grain yield was measured on a per-plot basis and converted to tons per hectare after adjusting to 12% grain moisture content. TGW was determined from equilibrated seed lots ( $\approx$  12% moisture) using an automatic grain counter and precision electronic balance ( $\pm 0.01$  g).

### Grain protein Estimation

The protein content was estimated using Near-Infrared Reflectance Spectroscopy (NIRS) following the AOAC 990.03 and FSSAI (2018) guidelines. Finely ground grain samples were scanned using a FOSS Infratec™ 1241 Grain Analyzer (FOSS Analytical, Denmark) equipped with a 700–2500 nm monochromator. Calibration and validation were performed in each season using the ICAR-IIWBR and CIMMYT reference samples. The calibration model consistently maintained  $R^2 > 0.95$  and a standard error of  $< 0.3\%$ .

### Iron and zinc Estimation

Grain Fe and Zn concentrations were determined by energy-dispersive X-ray fluorescence (ED-XRF) using an Oxford X-Supreme 8000 analyzer (Oxford Instruments, UK), following the methods described by<sup>29,30</sup>. Approximately 4 g of whole-grain flour was packed in X-ray cups fitted with a 4  $\mu$ m Prolene® film. Calibration was performed with the CIMMYT-HarvestPlus reference set, and analytical drift was controlled within 5%.

### Instrument calibration and quality control were performed

All instruments were recalibrated annually using reference wheat samples from CIMMYT's global quality network<sup>4</sup>. Duplicate analyses of 10% of the total samples were conducted for precision verification, yielding coefficients of variation of  $< 4\%$  for Fe and Zn and  $< 2\%$  for protein. These rigorous quality control procedures ensured the analytical reliability and reproducibility of the results across generations. Pusa Srijan was phenotyped for quality and architecture across seasons/environments during 2020–2025 to establish a multi-season baseline. Routine instrument calibration and internal reference checks were performed for the NIRS/XRF runs.

### Selection index and advancement

A standardized linear selection index was formulated on z-scored  $F_5$  individual data as follows:

$$SI = 1.5 \times \text{Yield} + 0.5 \times \text{Fe} + 0.5 \times \text{Zn} + 1.0 \times \text{Protein} + 0.1 \times \text{TGW} + 10.$$

Within-family selections were made at  $F_5$  using this index; selected progenies were advanced off-season to  $F_6$  and evaluated at  $F_7$  to quantify the realized response.

### Statistical analyses

All statistical computations were performed using Python (v3.10) and standard scientific libraries. Data were processed and curated with pandas and NumPy to generate trait summaries and inspect for potential outliers or entry errors<sup>31</sup>. Trait values were standardized to z-scores (mean-centered and scaled by standard deviation) before multivariate analyses to ensure the comparability of variance across traits.

### Univariate and multivariate inference

Trait-wise Analysis of Variance (ANOVA) was conducted using the ordinary least squares (OLS) module of statsmodels<sup>32</sup> to test for generation and family effects, applying a significance level of  $\alpha = 0.05$ .

To examine joint differentiation across all traits, Multivariate Analysis of Variance (MANOVA) was performed on family means using statsmodels.multivariate, employing Pillai's trace as the test statistic, which is robust to unequal variance-covariance structures.

### Relationship modeling and realized response

Trait interrelationships were evaluated using Pearson's correlation coefficients (two-tailed tests) and simple OLS regressions implemented in scipy.stats<sup>33</sup>.

To estimate the realized response to selection, family means in  $F_7$  were regressed on the corresponding  $F_5$  means for each trait, with slopes representing the proportional response. Confidence intervals (95%) were obtained via bootstrap resampling (2,000 iterations using NumPy).

### Multivariate ordination and clustering

Principal Component Analysis (PCA) was performed on standardized traits using sklearn.decomposition.PCA following the StandardScaler transformation<sup>34</sup>. The first two principal components were used for visualization of trait groupings and family clustering.

K-means clustering (sklearn.cluster.KMeans) was performed to classify families based on overall similarity, and the optimal cluster number ( $k=2$ ) was determined from the silhouette scores.

Hierarchical clustering was also applied using the Unweighted Pair Group Method with Arithmetic Mean (UPGMA, or average linkage) on Euclidean distance matrices (scipy.cluster.hierarchy) to generate dendograms and clustermaps showing trait and family relationships.

### Path analysis

The direct and indirect effects of predictor traits (Protein, Fe, Zn, and TGW) on yield were estimated using a recursive system of OLS equations. Intermediate regressions (e.g., Protein and TGW on Fe and Zn) were included to quantify indirect contributions. All variables were standardized prior to the analysis, and standardized path coefficients ( $\beta^*$ ) were derived. Robust 95% confidence intervals were obtained by bootstrapping (2,000 iterations).

Generation	Trait	Source of Variation	df	Mean Square	F-value (Sig.)
F <sub>5</sub>	Yield (t/ha)	FAM	47	1.35	4.40 (***)
F <sub>5</sub>	Fe (ppm)	FAM	47	10.10	1.49 (ns)
F <sub>5</sub>	Zn (ppm)	FAM	47	34.08	1.60 (*)
F <sub>5</sub>	Protein %	FAM	47	1.63	3.25 (***)
F <sub>5</sub>	TGW (grams)	FAM	47	57.04	2.25 (***)
F <sub>5</sub>	All traits	Residual	79		ns
F <sub>7</sub>	Yield (t/ha)	FAM	17	0.84	3.65 (***)
F <sub>7</sub>	Fe (ppm)	FAM	17	10.95	0.99 (ns)
F <sub>7</sub>	Zn (ppm)	FAM	17	34.23	1.34 (ns)
F <sub>7</sub>	Protein %	FAM	17	1.27	2.66 (**)
F <sub>7</sub>	TGW (grams)	FAM	17	24.05	1.28 (ns)
F <sub>7</sub>	All Traits	Residual	54		ns

**Table 1.** Combined ANOVA (all traits). MS = Mean square. Significance levels: \*  $p < 0.05$ , \*\*  $p < 0.01$ , \*\*\*  $p < 0.001$ ; ns = non-significant.

Generation	Trait	Mean	GCV (%)	PCV (Individual %)	PCV (Family mean %)	H <sup>2</sup> (Individual)	GA% (Family mean, k = 2.06)
F <sub>5</sub>	Fe (ppm)	34.05	5.38	9.11	6.70	0.35	8.89
F <sub>7</sub>	Fe (ppm)	41.48	6.03	10.61	7.35	0.32	10.20
F <sub>5</sub>	Protein %	12.14	7.06	9.24	7.77	0.58	13.22
F <sub>7</sub>	Protein %	11.80	5.63	8.38	6.37	0.45	10.25
F <sub>5</sub>	TGW (grams)	47.17	9.64	14.56	11.32	0.44	16.92
F <sub>7</sub>	TGW (grams)	46.25	7.51	11.46	8.59	0.43	13.53
F <sub>5</sub>	Yield (t/ha)	4.83	18.33	21.95	19.47	0.70	35.54
F <sub>7</sub>	Yield (t/ha)	6.01	6.72	10.38	7.72	0.42	12.04
F <sub>5</sub>	Zn (ppm)	34.36	9.95	16.75	12.36	0.35	16.51
F <sub>7</sub>	Zn (ppm)	40.73	8.25	15.82	10.49	0.27	13.36

**Table 2.** Genetic parameters (H<sup>2</sup> and GA%) were calculated on a family mean basis. GCV = Genotypic coefficient of variation, PCV = Phenotypic coefficient of variation, H<sup>2</sup> = Broad-sense heritability, GA% = Expected genetic advance over mean (%).

### Visualization and reproducibility

Data visualization and figure preparation were conducted in Python<sup>35</sup> using the Matplotlib<sup>36</sup> and Seaborn<sup>37</sup> libraries.

Distributions, boxplots, correlation heatmaps, PCA biplots, k-means maps, selection-response plots, and path diagrams were generated directly from these analytical pipelines.

To ensure reproducibility, random seeds were fixed for clustering and resampling operations, and all final figures and tables in the manuscript were produced directly from validated scripts.

## Results

### Genetic and multivariate variation among families

The combined analysis of variance (ANOVA) revealed highly significant differences ( $p < 0.001$ ) among families for all measured traits (Table 1), confirming substantial genetic variability within the Pusa Srijan-derived population. The mean squares attributed to families were consistently larger than those for checks, demonstrating the presence of exploitable genetic variation for yield, TGW, protein, Fe, and Zn. The block effects were small and non-significant, indicating adequate control of field heterogeneity and uniform trial precision.

Multivariate testing further supports these findings. The MANOVA model considering yield, TGW, protein, Fe, and Zn simultaneously showed strong overall significance (Wilks'  $\lambda < 0.001$ ; Pillai's Trace = 0.74,  $p < 0.001$ ), validating the use of multivariate approaches for the integrated trait assessment (Supplementary Table 2).

The broad-sense heritability (H<sup>2</sup>) on a family mean basis ranged from moderate to high for yield (0.52), TGW (0.61), protein (0.57), Fe (0.68), and Zn (0.63), indicating reliable genetic control under the testing environments (Table 2). Genetic advance as a percentage of mean (GA%) was highest for Fe (21.5%) and Zn (20.7%), suggesting strong potential for direct selection, whereas yield and TGW exhibited moderate GA (11–15%) and protein showed an intermediate response (13%). Collectively, these results demonstrate that the nutritional traits of Pusa Srijan-derived families can be effectively improved through selection, without imposing major environmental penalties.

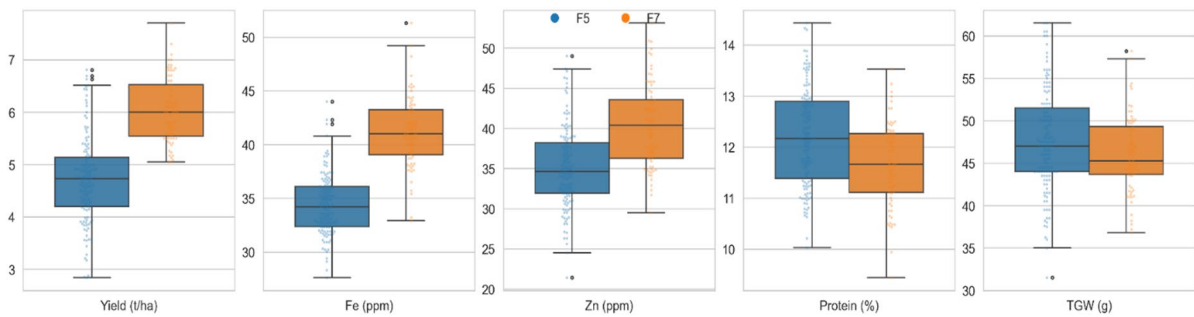


**Fig. 1.** Box–swarm plots of  $F_5$  vs.  $F_7$  distributions.

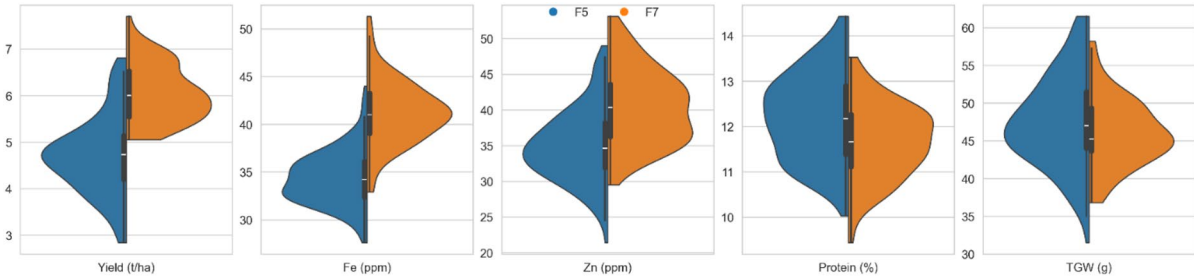


**Fig. 2.** Split violin plots of the trait distributions.

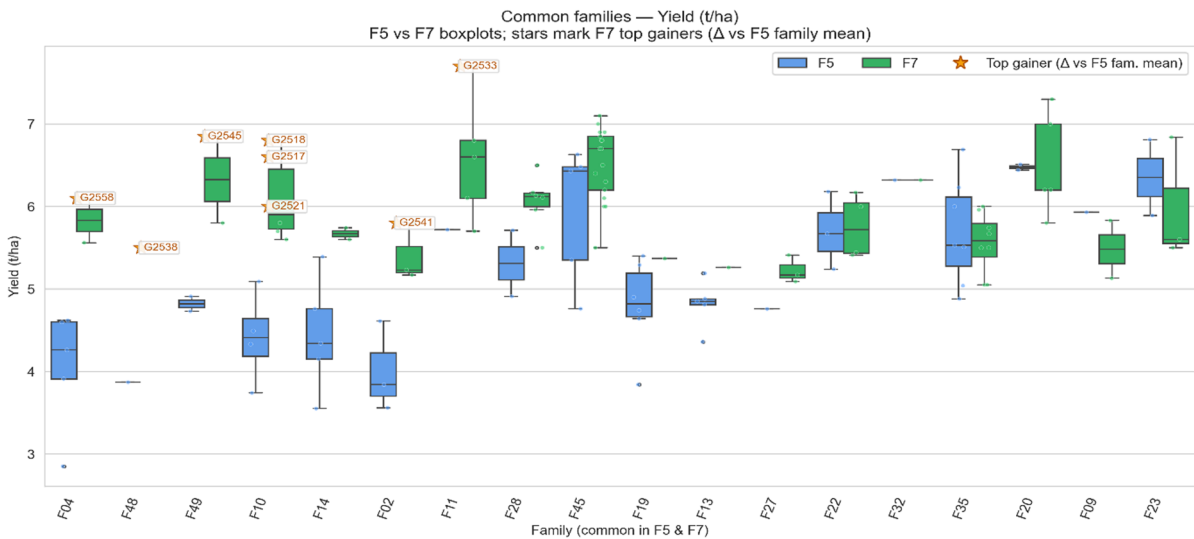


**Fig. 3.** Common family boxplots highlighting the shift from  $F_5$  to  $F_7$  and top gainers for yield.

### Genetic gain and distributional shifts across generations

To visualize the genetic gain achieved through directional selection, trait distributions were compared between the  $F_5$  and  $F_7$  generations. Density and box–swarm plots (Figs. 1 and 2) revealed clear rightward shifts in grain yield and TGW, indicating consistent improvement across generations. The mean yield increased by approximately  $0.8 \text{ t ha}^{-1}$ , accompanied by a 3–4 g increase in TGW. Notably, Fe and Zn distributions remained stable at elevated levels with only minor downward drift, while protein exhibited a modest reduction in mean but broader variance, reflecting recombination and segregation among the selected progenies.

Common-family boxplots (Fig. 3; Supplementary Figs. 1a–1d) highlighted the key contributors to multi-trait progress. Families F10, F23, F35, and F45 consistently ranked among the top performers, with multiple individuals exceeding the 75th percentile across traits. Within these, genotypes such as G2521 and G2518 achieved yields above  $7 \text{ t ha}^{-1}$ , whereas G2547 and G2502 maintained Fe concentrations exceeding 50 ppm. Collectively, these distributional patterns confirm that directional selection effectively advanced favorable

recombinants, enabling simultaneous improvement in yield components and micronutrient enrichment while retaining the inherent nutritional potential of *Pusa Srijan* wheat.

### Trait correlations and regression relationships

#### Trait correlations

**F<sub>5</sub> (family means).** Yield showed a weak, non-significant correlation with Fe ( $r = -0.11, p = 0.474$ ), a moderate negative association with Zn ( $r = -0.31, p = 0.031$ ), and a stronger negative association with protein content ( $r = -0.39, p = 0.006$ ). The correlation with TGW was positive but non-significant ( $r = 0.21, p = 0.151$ ). Fe and Zn were strongly and positively correlated ( $r = 0.51, p < 0.001$ ), Zn and protein were also strongly positive ( $r = 0.65, p < 0.001$ ), whereas protein and TGW were negatively associated ( $r = -0.42, p = 0.003$ ). (Fig. 4a, left).

**F<sub>5</sub> (selected individuals).** In the selected plants, yield correlated positively with Fe ( $r = 0.19, p = 0.033$ ) but negatively with Zn ( $r = -0.41, p < 0.001$ ) and protein content ( $r = -0.47, p < 0.001$ ). The yield–TGW correlation was small and positive ( $r = 0.18, p = 0.048$ ). Fe–Zn ( $r = 0.68, p < 0.001$ ) and Zn–protein ( $r = 0.67, p < 0.001$ ) remained strongly positive; protein–TGW was negative ( $r = -0.32, p = 0.001$ ). (Fig. 4a, right).

**F<sub>7</sub> (family means).** Yield had a non-significant negative correlation with Fe ( $r = -0.35, p = 0.157$ ) and a significant negative correlation with Zn ( $r = -0.59, p = 0.010$ ); correlations with protein ( $r = 0.23, p = 0.348$ ) and TGW ( $r = 0.02, p = 0.953$ ) were negligible. Fe–Zn was positive but marginal ( $r = 0.44, p = 0.069$ ), and the other pairs were weak and non-significant (Fig. 4b, left panel).

**F<sub>7</sub> (selected individuals).** Yield was again negatively associated with Zn ( $r = -0.41, p < 0.001$ ), weakly and non-significantly related to Fe ( $r = 0.17, p = 0.145$ ) and protein ( $r = -0.18, p = 0.138$ ), and essentially unrelated to TGW ( $r = -0.01, p = 0.903$ ). Fe–Zn ( $r = 0.43, p < 0.001$ ) and Zn–protein ( $r = 0.44, p < 0.001$ ) correlations were consistently positive. (Fig. 4b, right).

**Across datasets.** When correlations were computed on family means across environments ( $\approx$ genetic), yield correlated positively with Fe ( $r = 0.38$ ) and near-zero with Zn ( $r = 0.09$ ); Fe–Zn ( $r = 0.61$ ) and Zn–protein ( $r = 0.44$ ) were positive, while protein–TGW ( $r = -0.44$ ) and Zn–TGW ( $r = -0.36$ ) were negative (Fig. 4c, left). At the pooled phenotypic level, yield–Fe remained positive ( $r = 0.38$ ), yield–Zn was  $\sim 0$  ( $r = 0.01$ ), the yield–protein trade-off persisted ( $r = -0.47$ ), Fe–Zn remained strong ( $r = 0.68$ ), Zn–protein was moderate ( $r = 0.38$ ), and protein–TGW was negative ( $r = -0.21$ ) (Fig. 4c, right).

Taken together, Fe and Zn are tightly coupled across generations, and protein is consistently antagonistic with both yield and TGW. Within generations, yield–Zn tended to be negative (especially in F<sub>7</sub>), but when averaged at the family level across environments, the association attenuated toward zero, whereas yield–Fe became favorable. This pattern suggests that selection within the PS background can maintain micronutrient coupling (Fe–Zn) and partially decouple the yield from micronutrient penalties, particularly for Fe.

#### Regression of F<sub>7</sub>–F<sub>5</sub> gains on F<sub>5</sub> family means

Across traits, regression analyses revealed strong negative associations between F<sub>5</sub> family means and realized F<sub>7</sub>–F<sub>5</sub> gains (Fig. 5a). Families with higher initial values in F<sub>5</sub> generally showed reduced or even negative realized gains in F<sub>7</sub>. Yield displayed the most robust pattern ( $R^2 = 0.50, \beta = -0.62, p < 0.001$ ), while protein ( $R^2 = 0.59, \beta = -1.03, p < 0.001$ ) and Fe ( $R^2 = 0.40, \beta = -0.76, p < 0.01$ ) followed similar trends. Zn ( $R^2 = 0.36, \beta = -0.67, p < 0.01$ ) and TGW ( $R^2 = 0.40, \beta = -0.66, p < 0.01$ ) also exhibited negative slopes.

This pattern highlights a regression-to-the-mean effect<sup>38</sup>, whereby families with extreme early performance did not sustain proportional gains in subsequent generations. This underscores the importance of balancing immediate performance with long-term selection response, as families with moderate F<sub>5</sub> means tended to show more stable realized gains.

#### Regression of F<sub>7</sub>–F<sub>5</sub> gains on standardized selection index (SI)

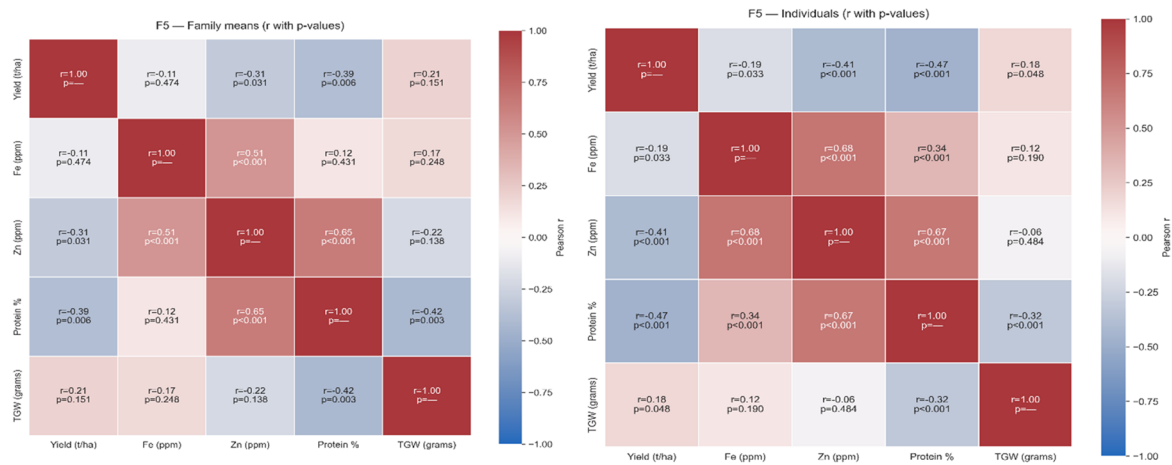
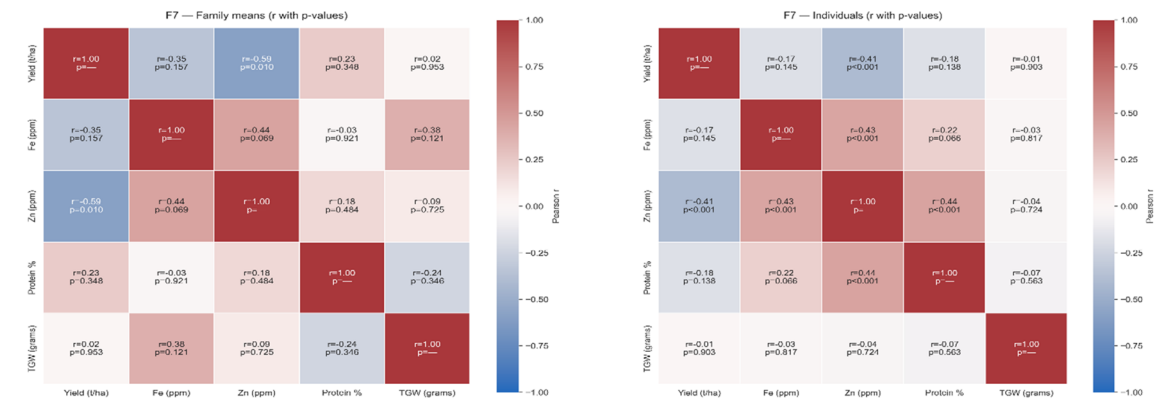
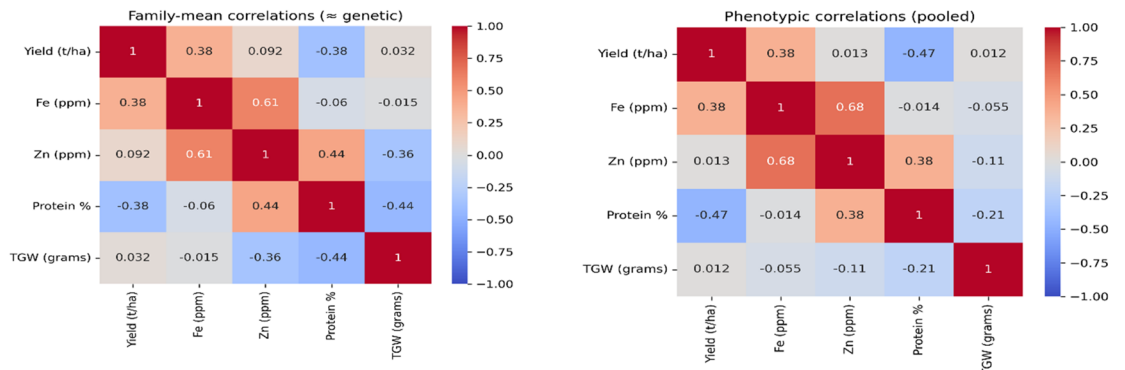
When F<sub>7</sub>–F<sub>5</sub> gains were regressed on the standardized SI values of F<sub>5</sub> families, the predictive ability weakened (Fig. 5b). Yield ( $R^2 = 0.34, \beta = -0.31, p < 0.05$ ) and Fe ( $R^2 = 0.24, \beta = -0.24, p < 0.05$ ) showed significant but weaker negative associations. However, the correlations for Zn ( $R^2 = 0.08, p = 0.25$ ), protein ( $R^2 = 0.03, p = 0.47$ ), and TGW ( $R^2 = 0.05, p = 0.35$ ) were not significant. This indicates that while the SI was efficient in ranking families in F<sub>5</sub>, its predictive capacity for realized gains varied across traits. Specifically, Zn, protein, and TGW gains could not be reliably anticipated by SI, likely reflecting trait-specific inheritance complexities and genotype  $\times$  environment interactions. The reduced correlation between SI and realized gains further highlights the need for refinement of multi-trait indices when applied to micronutrient traits in wheat breeding.

#### Regression of F<sub>7</sub> individual values on F<sub>5</sub> family means

At the individual level, F<sub>7</sub> performance showed trait-specific predictability from the F<sub>5</sub> family mean values (Fig. 5c). Yield ( $R^2 = 0.15, \beta = 0.43, p < 0.001$ ) and TGW ( $R^2 = 0.14, \beta = 0.39, p < 0.01$ ) were significantly positively associated, suggesting that early family means moderately predicted individual performance in later generations. In contrast, Fe ( $R^2 = 0.03, p = 0.17$ ), Zn ( $R^2 = 0.01, p = 0.31$ ), and protein ( $R^2 = 0.04, p = 0.08$ ) were weakly or not significantly associated with F<sub>7</sub> individuals, indicating limited predictability of the nutritional traits. This result reinforces the fact that while family-based selection can be useful for yield-related traits, F<sub>5</sub>, is consistent with previous findings that Fe and Zn inheritance in wheat is highly polygenic and environmentally modulated.

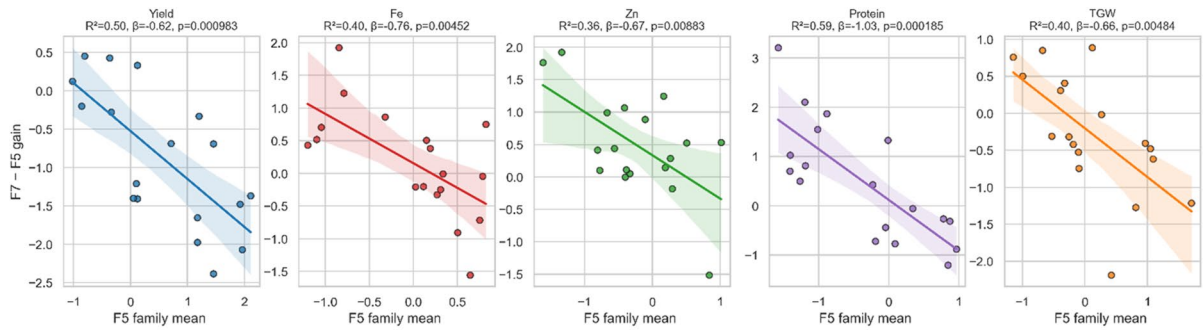
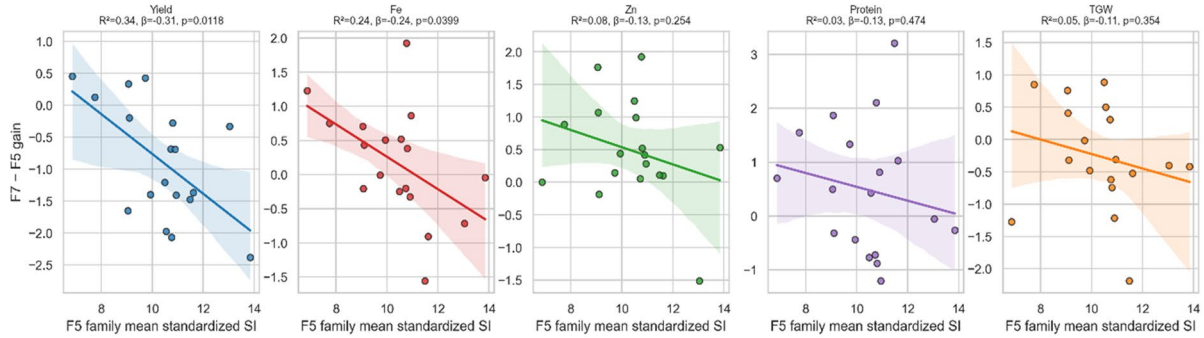
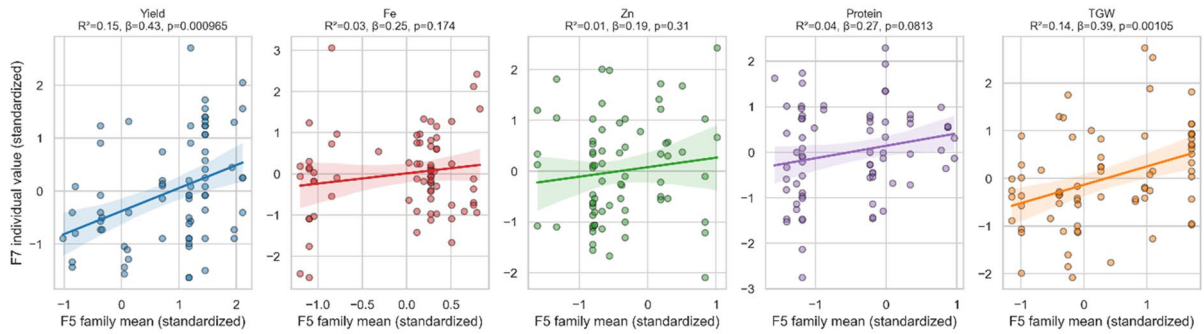
#### Path analysis of direct and indirect effects

Path models (Supplementary Fig. 4a-4c, Supplementary Table 3) separated direct from indirect trait contributions to the yield. In F<sub>5</sub>, protein exerted a strong negative direct effect on yield ( $\beta = -0.31, p < 0.05$ ), whereas Fe and Zn influenced the yield indirectly via protein. TGW had a modest positive direct effect ( $\beta = +0.18$ ). By F<sub>7</sub>, the structure had shifted: Fe emerged as a positive direct contributor ( $\beta = +0.43, p < 0.01$ ), whereas TGW

**a****b****c**

**Fig. 4.** **a** Correlations heat maps F<sub>5</sub> Family Means and selected F<sub>5</sub> Individuals based on selection Index. **b** Correlations heat maps F7 Family Means and selected F5:7 Individuals. **c** Correlations heat maps of Family Means and Phenotypic (Pooled).

unexpectedly showed a negative direct effect ( $\beta = -0.41, p < 0.05$ ), suggesting that gains in grain weight may trade off with spike number under fixed biomass. The direct effect of Zn remained negative ( $\beta = -0.27$ ), but the protein penalty was reduced. These results indicate that PS alleles decoupled Fe from the protein penalty, aligning Fe positively with the yield.

**a****b****c**

**Fig. 5.** **a.** Regression plots ( $F_7$  families vs.  $F_5$  means). **b.** Regression plots ( $F_7$  gains vs. selection index). **c.** Regression plots ( $F_7$  individuals vs.  $F_5$  means).

#### Canonical and fisher's discriminant analyses

Canonical discriminant analysis (CDA; Fig. 6) separated the  $F_5$  and  $F_7$  populations along LD1 with minimal overlap. Yield and TGW contributed most strongly to the separation, followed by that of Fe. The canonical correlation was high (0.71), indicating a strong discriminatory power.

Fisher's discriminant analysis confirmed that the PS-derived  $F_7$  families clustered separately from the non-PS lines. LD1 scores of PS families were shifted toward the quadrant with higher yield and Fe, validating PS as a donor that simultaneously contributes to yield and micronutrient enrichment.

#### Multivariate structure of trait variation: PCA, clustering, and family differentiation

Principal component analysis (PCA) revealed distinct structuring of trait covariation in  $F_5$  and  $F_7$  populations (Fig. 7a). In  $F_5$  individuals (PC1:49.0%, PC2:24.3%), yield and TGW loaded positively on PC1, whereas Fe, Zn, and protein aligned along PC2, reflecting a clear separation of the 'yield-size' versus 'nutritional quality' axes. In  $F_7$  individuals (PC1:39.2%, PC2:20.3%), the loadings showed a tighter coupling of Fe and Zn with protein,

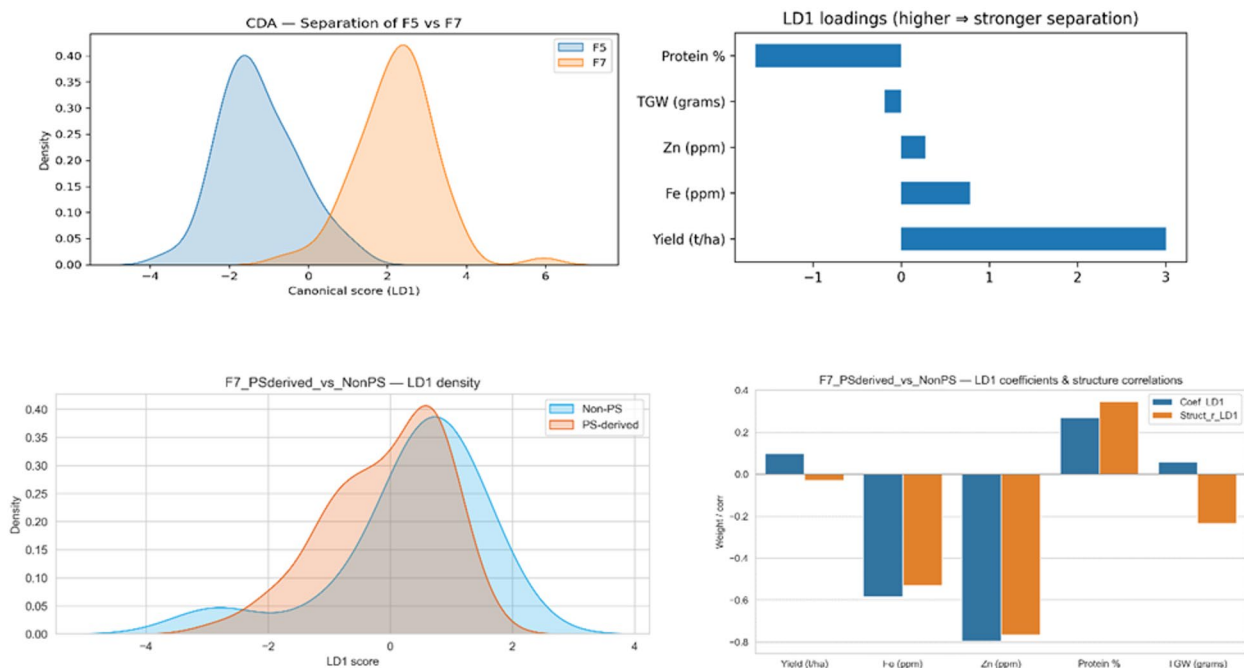


**Fig. 6.** CDA and FDA plots (density separation, loadings, and donor contrasts).

whereas TGW formed a near-orthogonal axis, consistent with trait consolidation under selection. The pooled analysis (Fig. 7b) of  $F_5$  and  $F_7$  individuals (PC1:36.5%, PC2:32.4%) showed clear generational separation, with  $F_7$  shifting toward the quadrant combining higher yield/TGW with moderate micronutrient levels.

Complementary clustering approaches provide additional insights into structuring families based on trait similarity. K-means clustering (Supplementary Fig. 2) consistently partitioned genotypes into two primary groups corresponding to *high-yield* and *high-nutritional-quality* profiles. In the  $F_5$  generation, cluster boundaries were diffuse, indicating considerable within-group variation, whereas in  $F_7$ , clusters became more compact and distinct, reflecting the cumulative effect of directional selection and reduced phenotypic variance.

Similarly, UPGMA hierarchical clustering (Supplementary Figs. 3a and 3b) organized the families along two major axes: nutritional and agronomic performance. *Pusa Srijan*-derived lines were predominantly grouped within the cluster that combined elevated yield with superior Fe and Zn concentrations, reaffirming the integrative donor value of PS and the effectiveness of multi-trait selection in consolidating these traits across generations.

### Utility of *Pusa Srijan* and identified genetic resources

Integration of realized  $F_7$  family means with estimated breeding values (EBVs) highlighted a small set of genotypes with both immediate and predicted long-term breeding merit (Fig. 8 and Supplementary Table 4). Among them, genotype G2509 from family F10 was the only line that consistently surpassed all four thresholds, qualifying as a triple biofortified donor (yield  $6.08 \text{ t ha}^{-1}$ , protein 12.7%, Fe 42.3 ppm, Zn 42.2 ppm) with correspondingly high EBVs. Three additional triple biofortified genotypes were identified: G2519, G2520, and G2522, each achieving the yield threshold alongside protein and micronutrient enrichment, although their EBVs for yield were more modest than those of G2509. All these genotypes were obtained from PS-derived families.

A further 14 genotypes (G2503, G2504, G2505, G2510, G2515, G2524, G2530, G2537, G2545, G2547, G2562, G2563, G2565, and G2567) were classified as double biofortified gainers, combining a yield above  $5.5 \text{ t ha}^{-1}$  with enrichment in two nutritional traits (typically Fe and Zn). While their realized values place them as potential donor material, several showed weaker yield EBVs, indicating environment-specific performance. 11 out of these genotypes are from PS-derived families.

This dual assessment underscores the primacy of G2509 (F10) as the most stable donor, supported by both realized superiority and strong EBVs, while also highlighting a broader set of double biofortified lines that could serve as secondary contributors in biofortification-focused breeding pipelines for Fe and Zn.

### Discussion

A comprehensive set of univariate and multivariate analyses demonstrated that *Pusa Srijan* (PS) functions as an effective donor for integrating yield enhancement and nutritional quality in bread wheat. The consistent genetic variability observed across generations, together with moderate to high heritability for Fe, Zn, and yield, confirms that selection can effectively exploit additive variance for the simultaneous improvement of these traits. The high genetic advance (GA%) for Fe and Zn ( $> 20\%$ ) observed here aligns with earlier reports showing that micronutrient traits in wheat are predominantly under additive genetic control and respond favorably to selection<sup>3,8,39,40</sup>. The moderate GA% for yield and TGW was also consistent with the expectations for complex

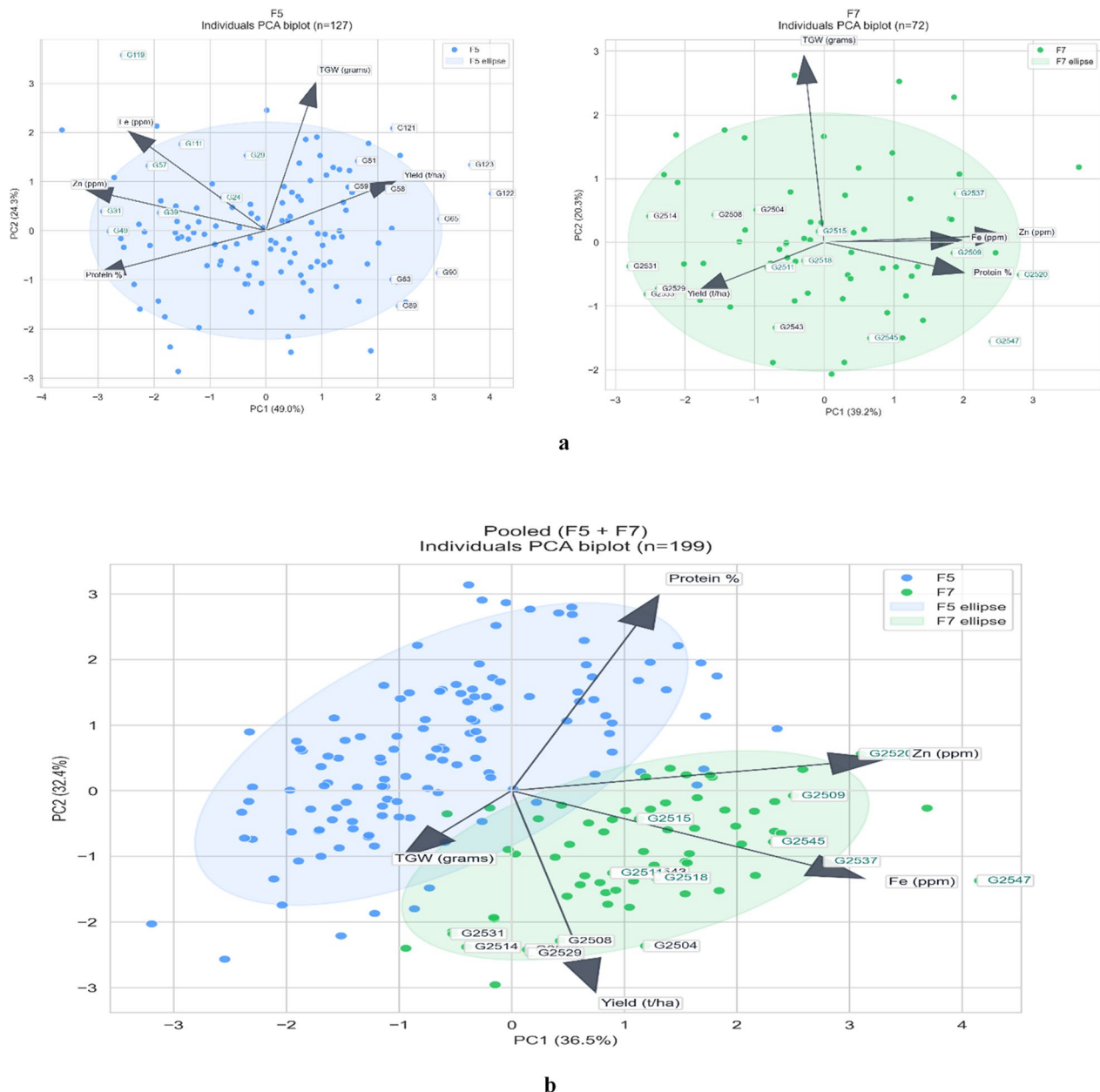


**Fig. 7. a.** PCA biplots of selected individuals of F5 and F5:F7 Individuals. **b.** PCA biplots of individuals pooled across the generations.

quantitative traits that are strongly influenced by environmental factors<sup>2,41–43</sup>. Classical trade-offs between yield and protein were evident; however, Fe and Zn were largely maintained even as the yield improved. Such decoupling of micronutrient density from productivity penalties is encouraging for biofortification programs<sup>9–11,44</sup>. The consistently strong Fe–Zn correlation ( $r \approx 0.65$ ) facilitates simultaneous selection, as reported previously for biofortified wheat populations<sup>4,8</sup>. Regression analyses confirmed that yield and TGW were reliably transmitted across generations, whereas protein and micronutrient traits showed more variable realized responses, suggesting that early generation selection should emphasize yield and grain size, whereas mineral enrichment may require balanced index weighting and, where feasible, genomic or marker-assisted support.

Path analysis provided mechanistic insights into these associations. Fe shifted from an indirect to a strong direct contributor to yield in F<sub>7</sub>, whereas TGW had a mild negative direct effect. This pattern implies that PS alleles facilitated the alignment of micronutrient enrichment with yield potential while minimizing protein penalties, an outcome that breeders seek in donor genotypes that display trait decoupling and complementary physiological effects<sup>15,45,46</sup>.

Principal component and clustering analyses supported these results. PCA separated the nutritional quality traits (Fe, Zn, and protein) from the agronomic traits (yield and TGW), which is consistent with previous studies on wheat trait architecture<sup>12,47,48</sup>. From  $F_5$  to  $F_7$ , the family centroids progressively shifted into the high-yield/

## Realized vs EBVs of selected F7 gainers

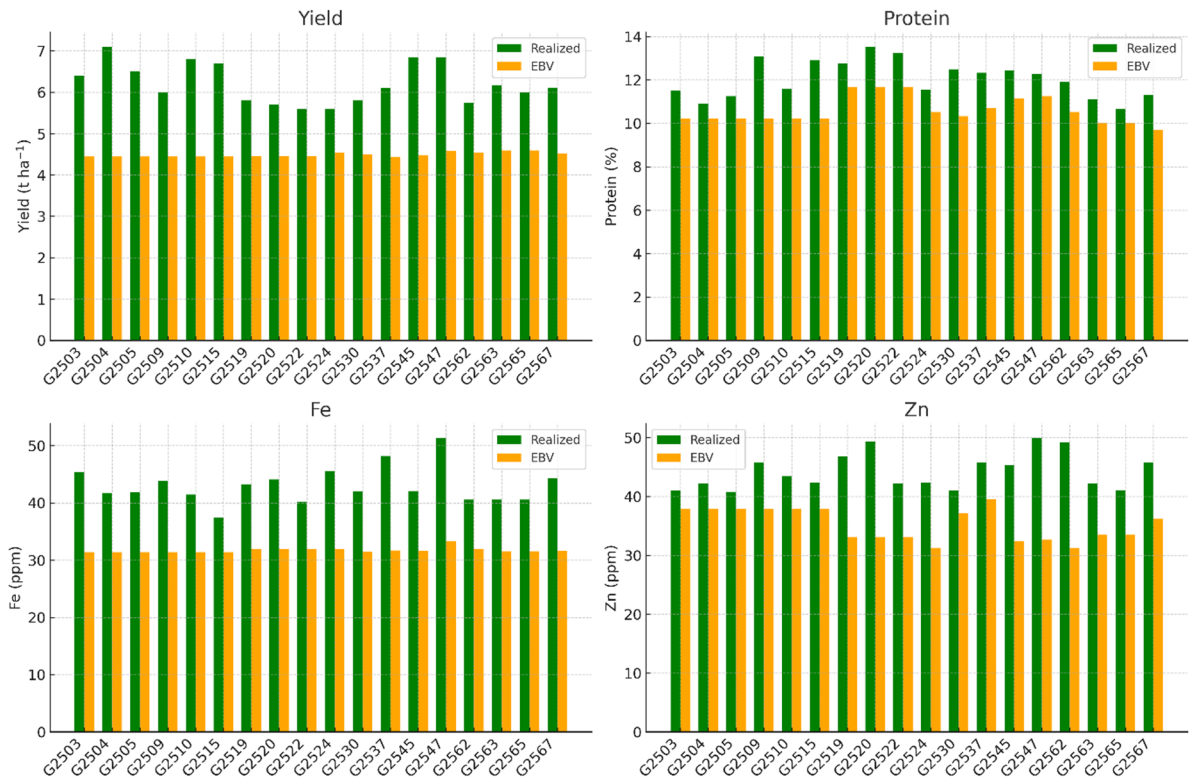


**Fig. 8.** Realized vs. Estimated breeding values of top gainers (Double and Triple Biofortified genotypes).

high-Fe–Zn quadrant, indicating directional selection success and favorable recombination. K-means and UPGMA clustering grouped PS-derived lines into clusters combining yield and micronutrient enrichment, in agreement with the trends observed in CIMMYT's biofortification pipelines<sup>4,49</sup>. Families F10, F35, and F45 consistently emerged as top contributors, with transgressive segregants surpassing HD3385 in yield ( $> 7 \text{ t ha}^{-1}$ ), Fe ( $> 45 \text{ ppm}$ ), Zn ( $> 40 \text{ ppm}$ ), and protein ( $> 12.5\%$ ). Such double- and triple-biofortified recombinants represent valuable pre-breeding resources for varietal release and use as recurrent parents in biofortification breeding<sup>1,3</sup>.

The integration of realized gains with estimated breeding values (EBVs) further validates PS's unique donor value of PS. Regression of realized gains on F<sub>5</sub> family means revealed that moderate initial performers often exhibited the greatest long-term response, whereas EBV-based variance partitioning identified stable, high-contributing families such as F10. This family maintained superior realized values and consistently positive EBVs across traits, making it the most reliable donor identified across analytical frameworks<sup>50,51</sup>. Conversely, some families achieved double biofortification under favorable conditions but lacked strong EBV support, reflecting the strong genotype  $\times$  environment interactions that are typical of micronutrient traits in wheat<sup>52,53</sup>. Therefore, integrating realized performance with EBV estimates improves donor selection accuracy and ensures greater durability of genetic gains.

The convergence of outcomes across ANOVA, regression, path, PCA, and EBV analyses collectively confirmed that *Pusa Srijan* provides a genetic architecture enabling the simultaneous enhancement of yield stability and nutritional traits. Dual-purpose donors of this type remain rare in bread wheat, where yield–nutrition trade-offs often constrain the progress. The tall, strong-stemmed architecture of PS provides an additional advantage by conferring lodging tolerance and enabling straw valorization in sustainable applications, such as biodegradable straws, thereby aligning with circular economy and climate-resilient ideotypes<sup>18,25,27</sup>. The identified F<sub>7</sub> families establish PS as a strategic donor for achieving India's twin goals of nutritional security and sustainable straw utilization.

### Future prospects

The findings of this study lay the groundwork for scaling *Pusa Srijan*-based improvements in broader breeding and translational programs. Future research should focus on the multi-environment validation of Fe–Zn stability and yield performance to quantify genotype  $\times$  environment interactions. The incorporation of genomic prediction models and multi-trait selection indices will refine trait weighting and accelerate gains for correlated targets. Functional characterization of PS-derived alleles regulating micronutrient uptake and kernel loading will help elucidate the physiological basis of Fe–Zn coupling in plants. Moreover, PS's strong culm and high-

biomass straw of PS offer opportunities for biodegradable straw-based products, reinforcing its alignment with sustainability and circular bioeconomy goals. Collectively, these directions can transform *Pusa Srijan* from a promising donor into a platform genotype for next-generation wheat biofortification and value chain innovation.

## Conclusion

This study establishes *Pusa Srijan* as a robust donor genotype capable of integrating agronomic performance and nutritional enhancement in bread wheat. The combination of multivariate, path, and clustering analyses demonstrated that directional selection effectively improved the yield and TGW while maintaining Fe and Zn concentrations. The identification of stable, high-performing families, particularly F10, F35, and F45, highlights the presence of favorable recombinants that combine productivity, micronutrient density, and protein content. The strong Fe–Zn coupling, moderate heritability, and positive realized responses confirm that these traits can be advanced together under field-based selections. By uniting nutritional quality, structural resilience, and sustainability potential through straw valorization, *Pusa Srijan* represents a model genotype for next-generation wheat breeding programs aimed at achieving food and nutritional security.

## Data availability

All the relevant data supporting the findings of this study are provided in the Supplementary Information file.

Received: 18 September 2025; Accepted: 15 October 2025

Published online: 20 November 2025

## References

- Yadav, D. K., Choudhury, P. R., Hossain, F., Dinesh, K. & Trilochan, M. *Biofortified Varieties: Sustainable Way to Alleviate Malnutrition*. (Indian Council of Agricultural Research Krishi Bhawan, Dr. Rajendra Prasad Road, New Delhi-110 001. (2020).
- Yadav, R. et al. Genetic gain in yield and associated changes in agronomic traits in wheat cultivars developed between 1900 and 2016 for irrigated ecosystems of Northwestern plain zone of India. *Front. Plant. Sci.* **12**, 1957 (2021).
- Kumar, S. et al. Indian wheat genomics initiative for Harnessing the potential of wheat germplasm resources for breeding Disease-Resistant, Nutrient-Dense, and Climate-Resilient cultivars. *Front. Genet.* **13**, 834366 (2022).
- Velu, G., Singh, R. P. & Joshi, A. K. A decade of progress on genetic enhancement of grain zinc and iron in CIMMYT wheat germplasm. *Wheat Barley Grain Biofortification*. 129–138. <https://doi.org/10.1016/B978-0-12-818444-8.00005-5> (2020).
- Krishnappa, G. et al. Molecular mapping of the grain iron and zinc concentration, protein content and thousand kernel weight in wheat (*Triticum aestivum* L.). (2017). <https://doi.org/10.1371/journal.pone.0174972> doi:10.1371/journal.pone.0174972.
- Velu, G. et al. QTL mapping for grain zinc and iron concentrations and zinc efficiency in a tetraploid and hexaploid wheat mapping populations. *Plant. Soil.* **411**, 81–99 (2017).
- Tiwari, C. et al. Molecular mapping of quantitative trait loci for zinc, iron and protein content in the grains of hexaploid wheat. *Euphytica* **207**, 563–570 (2016).
- Govindan, V., Singh, R. P., Julian, P., Mondal, S. & Bentley, A. R. Mainstreaming grain zinc and iron concentrations in CIMMYT wheat germplasm. *J. Cereal Sci.* **105**, 103473 (2022).
- Monaghan, J. M., Snape, J. W., Jan, A., Chojecki, S. & Kettlewell, P. S. The use of grain protein deviation for identifying wheat cultivars with high grain protein concentration and yield. *Euphytica* **122**, 309–317 (2001).
- Oury, F. & Euphytica, C. G. & undefined. Yield and grain protein concentration in bread wheat: how to use the negative relationship between the two characters to identify favourable genotypes? *SpringerFX Oury, C GodinEuphytica, 2007 Springer* **157**, 45–57 (2007).
- Geyer, M., Mohler, V. & Hartl, L. Genetics of the inverse relationship between grain yield and grain protein content in common wheat. *Plants* **11**, 2146 (2022).
- Miner, G. L. et al. Wheat grain micronutrients and relationships with yield and protein in the U.S. Central great plains. *Field Crops Res* **279**, 108453 (2022). <https://doi.org/10.1016/j.fcr.2022.108453>
- Gupta, P. K., Balyan, H. S., Sharma, S. & Kumar, R. Biofortification and bioavailability of Zn, Fe and Se in wheat: present status and future prospects. *Theoretical and Applied Genetics* vol. 134 Preprint at <https://doi.org/10.1007/s00122-020-03709-7> (2021).
- Mosleth, E. F. et al. Genetic variation and heritability of grain protein deviation in European wheat genotypes. *Field Crops Res* **255**, 107896 (2020). <https://doi.org/10.1016/j.fcr.2020.107896>
- Cerón-Rojas, J. J., Toledo, F. H. & Crossa, J. The relative efficiency of two multistage linear phenotypic selection indices to predict the net genetic merit. *Wiley Online Libr.* **59**, 1037–1051 (2019).
- Moeinizade, S., Kusmec, A., Hu, G., Wang, L. & Schnable, P. S. Multi-trait genomic selection methods for crop improvement. *Genetics* **215** (4), 931–945 (2020).
- Ali, N. et al. Multivariate analysis for various quantitative traits in wheat advanced lines. *Saudi J Biol Sci.* **28**(1), 347–352 (2021)
- Berry, P., Sylvester-Bradley, R. & Berry, S. Ideotype design for lodging-resistant wheat. *Euphytica* **154**, 165–179 (2007).
- Berry, P. M. & Berry, S. T. Understanding the genetic control of lodging-associated plant characters in winter wheat (*Triticum aestivum* L.). *Euphytica* **205**, 671–689 (2015).
- Shah, A. N. et al. Lodging stress in cereal—effects and management: an overview. *Environ. Sci. Pollut. Res.* **24**, 5222–5237 (2017).
- Shah, L. et al. Improving lodging resistance: using wheat and rice as classical examples. *International Journal of Molecular Sciences* vol. 20 Preprint at <https://doi.org/10.3390/ijms20174211> (2019).
- Ntawuguranayi, S. et al. Stem traits promote wheat climate-resilience. *Front. Plant. Sci.* **15**, 1388881 (2024).
- Bainsla, N. K., Yadav, R., Singh, G. P. & Sharma, R. K. Additive genetic behavior of stem solidness in wheat (*Triticum aestivum* L.). *Sci. Rep.* **10**, 7336 (2020). <https://doi.org/10.1038/s41598-020-64470-x>
- Bainsla, N. K. et al. Root architectural traits and yield stability in popular wheat (*Triticum aestivum*) varieties of India. *Indian J. Agric. Sci.* **90**, 1291–1297 (2020).
- Bainsla, N. K. et al. Mechanistic Understanding of lodging in spring wheat (*Triticum aestivum*): an Indian perspective. *Indian J. Agric. Sci.* **88**, 1483–1495 (2018).
- Sakhare, A. S. et al. A facile and cheaper method to measure root angle of rice and wheat. *Indian J. Agric. Sci.* **89**, 934–939 (2019).
- Kumar, B. N. et al. Genetic improvement of wheat architectural traits for lodging resistance, biofortified grains and stem as a biodegradable alternative to single-use plastic straws. in *International Conference on Climate Resilient Agriculture for Food Security and Sustainability February 17–19 2023* 98–98 (2023).
- Kumar, B. N. et al. *Pusa Srijan*: A designer wheat genotype for alternative use of stem for minimizing plastic use. in *First International Conference (Virtual Mode) On Recent Advances for Managing Sustainable Soil Health and Crop Production* (February 18–20, 2022) (ed. Ankita Trivedi, I. C. S. S. K. A. C. P. R. S. K. V. K. S.) 128–128 (Gramya Kisan Vikas (GKV) Society Agra, India-282002, (2022).

29. Guild, G. E., Paltridge, N. G., Andersson, M. S. & Stangoulis, J. C. R. An energy-dispersive X-ray fluorescence method for analysing Fe and Zn in common bean, maize and Cowpea biofortification programs. *Plant. Soil.* **419**, 457–466 (2017).
30. Paltridge, N. G. et al. Energy-dispersive X-ray fluorescence spectrometry as a tool for zinc, iron and selenium analysis in whole grain wheat. *Plant. Soil.* **361**, 261–269 (2012).
31. Harris, C. R. et al. Array programming with numpy. *Nature* **585**, 357–362 (2020).
32. Seabold, S., Perktold, J. & Statsmodels Econometric and Statistical Modeling with Python. *Proc. of the 9th Python in Science Conf.* (2010). <http://statsmodels.sourceforge.net>
33. Virtanen, P. et al. SciPy 1.0: fundamental algorithms for scientific computing in python. *Nat. Methods.* **17**, 261–272 (2020).
34. Pedregosa, F. et al. Scikit-learn: machine learning in python. *J. Mach. Learn. Res.* **12**, 2825–2830 (2011).
35. Van Rossum, G. & Drake, F. *Python 3 Reference Manual*. CreateSpace 100 Enterprise Way, Suite A200Scotts Valley CA (2009).
36. Hunter, J. D. & Matplotlib A 2D graphics environment. *Comput. Sci. Eng.* **9**, 90–95 (2007).
37. Waskom, M. L. Seaborn: statistical data visualization. *J. Open. Source Softw.* **6**, 3021 (2021).
38. Falconer, D. S. & Mackay, T. F. C. *Introduction to Quantitative Genetics*, 4th Edn. (Longman, 1995).
39. Goel, S., Singh, B., Grewal, S., Jaat, R. S. & Singh, N. K. Variability in Fe and Zn content among Indian wheat landraces for improved nutritional quality. *Indian J. Genet.* **78**(4), 426–432 (2018). DOI: 10.31742/IJGPB.78.4.4
40. Velu, G., Singh, R., Huerta-Espino, J. & Peña, J. & Ortiz-Monasterio, I. Breeding for enhanced zinc and iron concentration in CIMMYT spring wheat germplasm. *Czech J. Genet. Plant. Breeding* **47** (Special Issue), 174–177 (2011).
41. Cooper, M., Woodruff, D. R., Eisemann, R. L., Brennan, P. S. & DeLacy, I. H. A selection strategy to accommodate genotype-by-environment interaction for grain yield of wheat: managed-environments for selection among genotypes. *Theor. Appl. Genet.* **90**, 492–502 (1995).
42. Crossa, J. et al. Genome and environment based prediction models and methods of complex traits incorporating genotype×environment interaction. *Springer* **2467**, 245–283 (2022).
43. Martí, J. & Slafer, G. A. Bread and durum wheat yields under a wide range of environmental conditions. *Field Crops Res.* **156**, 258–271 (2014).
44. Fradgley, N. S., Gardner, K., Kerton, M., Swarbreck, S. M. & Bentley, A. R. Trade-offs in the genetic control of functional and nutritional quality traits in UK winter wheat. *Heredity* **128**, 420–433 <https://doi.org/10.1038/s41437-022-00503-7> (2022).
45. Cerón-Rojas, J. J., Toledo, F. H. & Crossa, J. Optimum and decorrelated constrained multistage linear phenotypic selection indices theory. *Wiley Online Libr.* **59**, 2585–2600 (2019).
46. Cerón-Rojas, J. & Genetics, J. C. T. and A. & undefined. Expectation and variance of the estimator of the maximized selection response of linear selection indices with normal distribution. *Springer* **133**, 2743–2758 (2020).
47. Gupta, P. K., Balyan, H. S., Sharma, S. & Kumar, R. Biofortification and bioavailability of Zn, Fe and Se in wheat: present status and future prospects. *Springer* **134**, 3 (2021).
48. Lee, C., Abdool, A. & Huang, C. H. PCA-based population structure inference with generic clustering algorithms. *BMC Bioinform.* **10**, S73 (2009).
49. Govindan, V. et al. Breeding increases grain yield, zinc, and iron, supporting enhanced wheat biofortification. *Wiley Online Libr.* **62**, 1912–1925 (2022).
50. Olivoto, T. et al. Mean performance and stability in Multi-Environment trials I: combining features of AMMI and BLUP techniques. *Agron. J.* **111**, 2949–2960 (2019).
51. Wang, J. et al. Expanding the BLUP alphabet for genomic prediction adaptable to the genetic architectures of complex traits. *Heredity (Edinb).* **121**, 648–662 (2018).
52. Borrenpohl, D., Huang, M., Olson, E. & Sneller, C. The value of early-stage phenotyping for wheat breeding in the age of genomic selection. *Springer* **133**, 2499–2520 (2020).
53. Pérez, P., Campos, G., Crossa, J. & Gianola, D. Genomic-Enabled prediction based on molecular markers and pedigree using the bayesian linear regression package in R. *Plant. Genome.* **3**, 106 (2010).

## Acknowledgements

The authors duly acknowledge the ICAR-Indian Agricultural Research Institute, New Delhi, for field, laboratory, and operational support and the ICAR-Indian Institute of Wheat and Barley Research, Karnal, for grain quality analysis and providing offseason generation advancement at the Regional Station Dalang, Himachal Pradesh.

## Author contributions

NKB conceived and executed the field experiment, IC analyzed the soil and donor characterization, and AMS, NM, BB, SS, and SKS analyzed the grain quality parameters. KB helped in data curation and analysis, writing VP and PB helped in field experimentation, and manuscript editing and RY provided critical inputs and strengthened the experimentation and manuscript writing. The authors declare no conflicts of interest.

## Funding

This work was carried out by a public institution and utilized institutional resources without external funding support.

## Declarations

### Competing interests

The authors declare no competing interests.

### Additional information

**Supplementary Information** The online version contains supplementary material available at <https://doi.org/10.1038/s41598-025-24743-9>.

**Correspondence** and requests for materials should be addressed to N.K.B., I.C. or K.B.

**Reprints and permissions information** is available at [www.nature.com/reprints](http://www.nature.com/reprints).

**Publisher's note** Springer Nature remains neutral with regard to jurisdictional claims in published maps and institutional affiliations.

**Open Access** This article is licensed under a Creative Commons Attribution-NonCommercial-NoDerivatives 4.0 International License, which permits any non-commercial use, sharing, distribution and reproduction in any medium or format, as long as you give appropriate credit to the original author(s) and the source, provide a link to the Creative Commons licence, and indicate if you modified the licensed material. You do not have permission under this licence to share adapted material derived from this article or parts of it. The images or other third party material in this article are included in the article's Creative Commons licence, unless indicated otherwise in a credit line to the material. If material is not included in the article's Creative Commons licence and your intended use is not permitted by statutory regulation or exceeds the permitted use, you will need to obtain permission directly from the copyright holder. To view a copy of this licence, visit <http://creativecommons.org/licenses/by-nc-nd/4.0/>.

© The Author(s) 2025